# Figures

## Figure captions

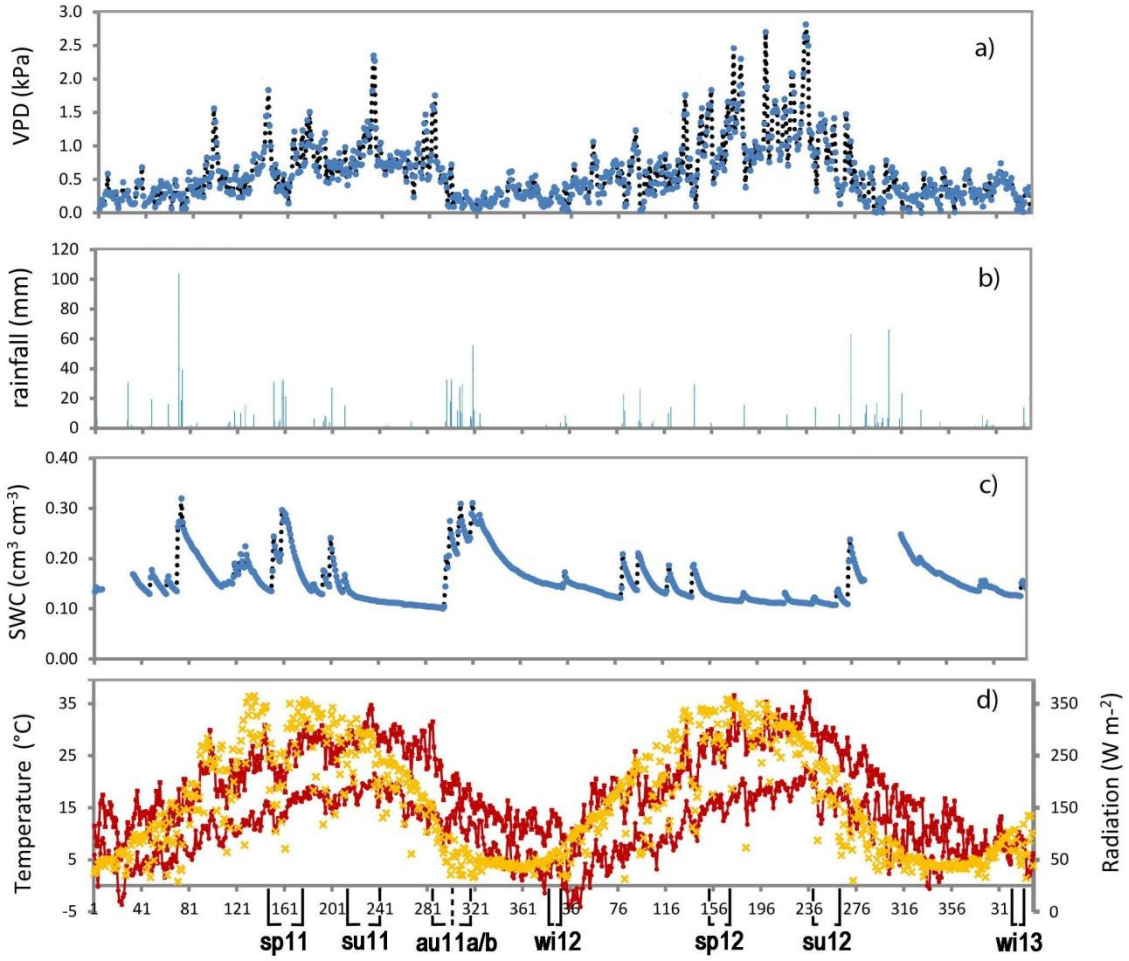


**Fig. 1.** Environmental variables are presented for the day of the year (DOY) from January 2011 until February 2013; a) atmospheric vapour pressure deficit (VPD), b) rainfall in mm c) soil water content in $cm^3\ cm^{-3}$ (gap in data is due to power cut), d) maximum and minimum temperatures in °C on the primary y-axes (in dark circles) and radiation in W $m^{-2}$ (in light crosses, foreground) on the secondary y-axes. Field campaigns are indicated (acronyms of seasons are detailed in Tab. 3).

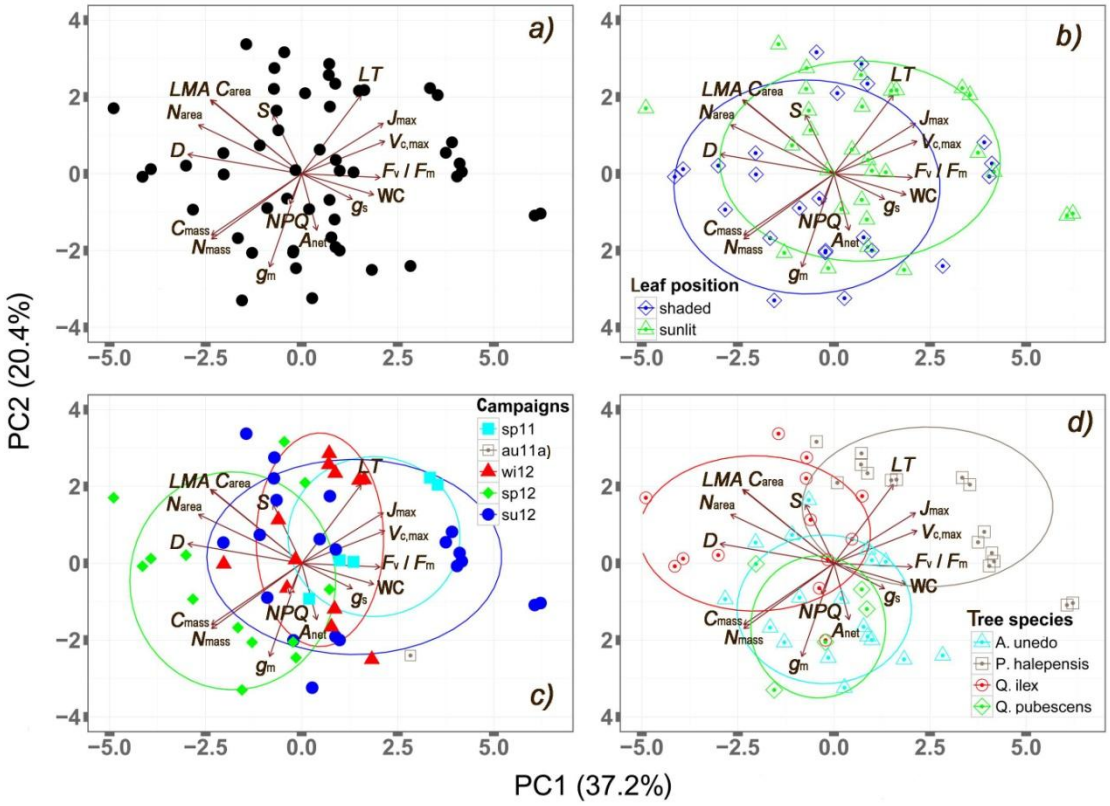


**Fig. 2.** Principal component analyses (PCA) for a) all trees species, leaf positions, and seasons, b) with differentiation between sunlit and shaded leaves, c) with differentiation between seasonal campaigns, and d) with differentiation between species. We used a subset of all data where both morphological and photosynthetic information was available. Fifteen parameters were used in the PCA: net assimilation rate ($A_{net}$), stomatal conductance ($g_s$), mesophyll conductance ($g_m$), maximum carboxylation rate ($V_{c,max}$), maximum electron transport rate ($J_{max}$), nonphotochemical quenching (NPQ), maximum quantum efficiency of PSII ($F_v/F_m$), leaf thickness (LT), leaf mass per area (LMA), leaf density (D), water content (WC), nitrogen content per leaf unit area ($N_{area}$), nitrogen content per leaf unit mass ($N_{mass}$), carbon content per leaf unit area ($C_{area}$), and carbon content per leaf unit mass ($C_{mass}$). The directions of the arrows indicate the higher levels of the parameters. Principal component (PC) 1 explains 37.2% of the variation, and PC 2 explained 20.4%. The ellipses are normal probability contour lines of 68% for the factors in b) leaf positions, c) seasons, and d) species.

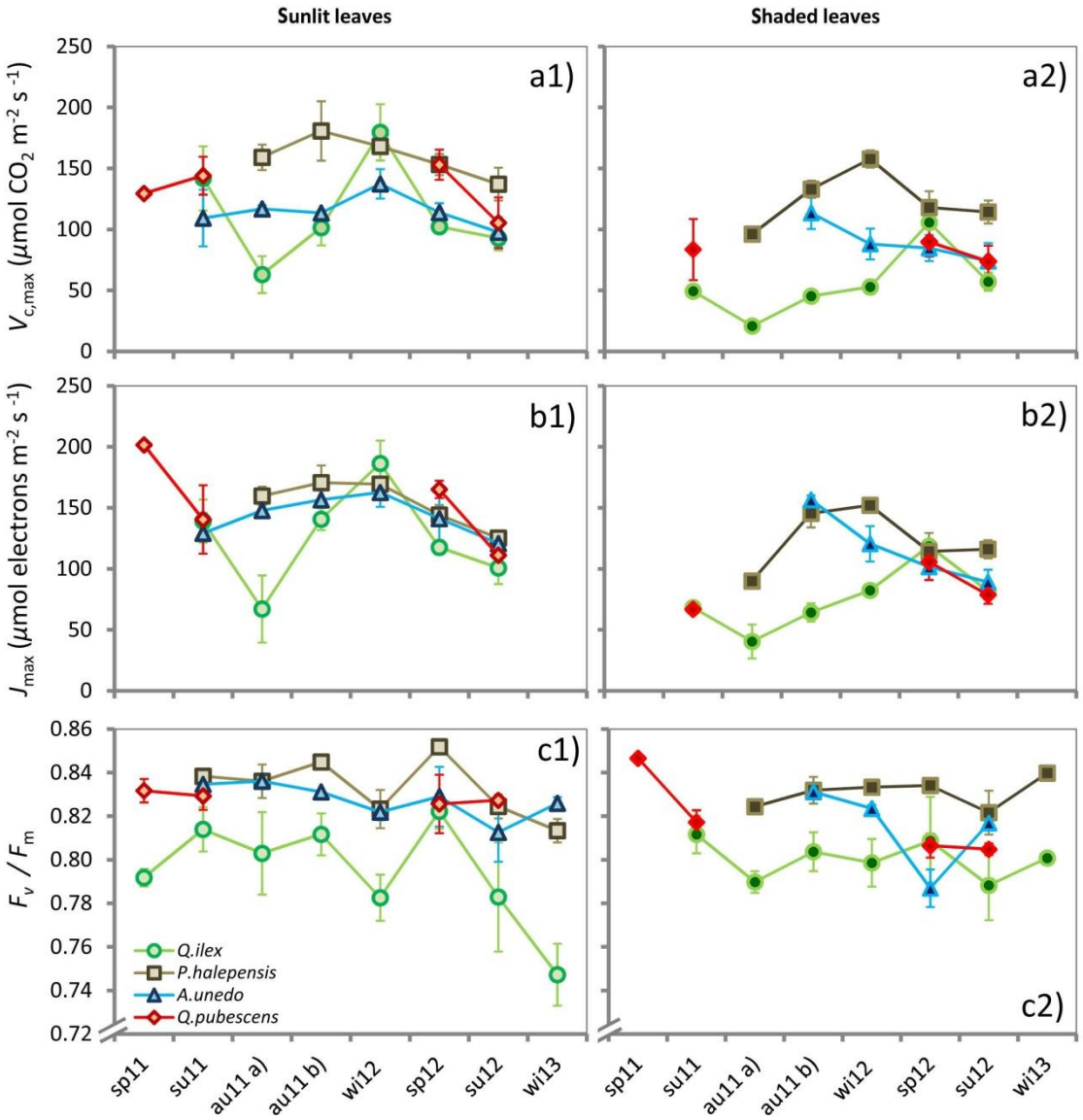


**Fig. 3.** Line graphs depicting seasonal changes of a) maximum carboxylation rate ($V_{c,max}$), b) maximum electron-transport rate ($J_{max}$), and c) maximum quantum efficiency of PSII ($F_v/F_m$) for *Q. ilex*, *P. halepensis*, *A. unedo*, and *Q. pubescens* in sunlit (1) and shaded (2) leaves. Seasonal campaigns were conducted in spring 2011 (sp11), summer 2011 (su11), autumn 2011[a] (au11 a), autumn 2011[b] (au11b), winter 2012 (wi12), spring 2012 (sp12), summer 2012 (su12), and winter 2013 (wi13). Missing data points were due to limitations of labour and equipment. Vertical bars indicate standard errors of the means ($n$ = 3-5).

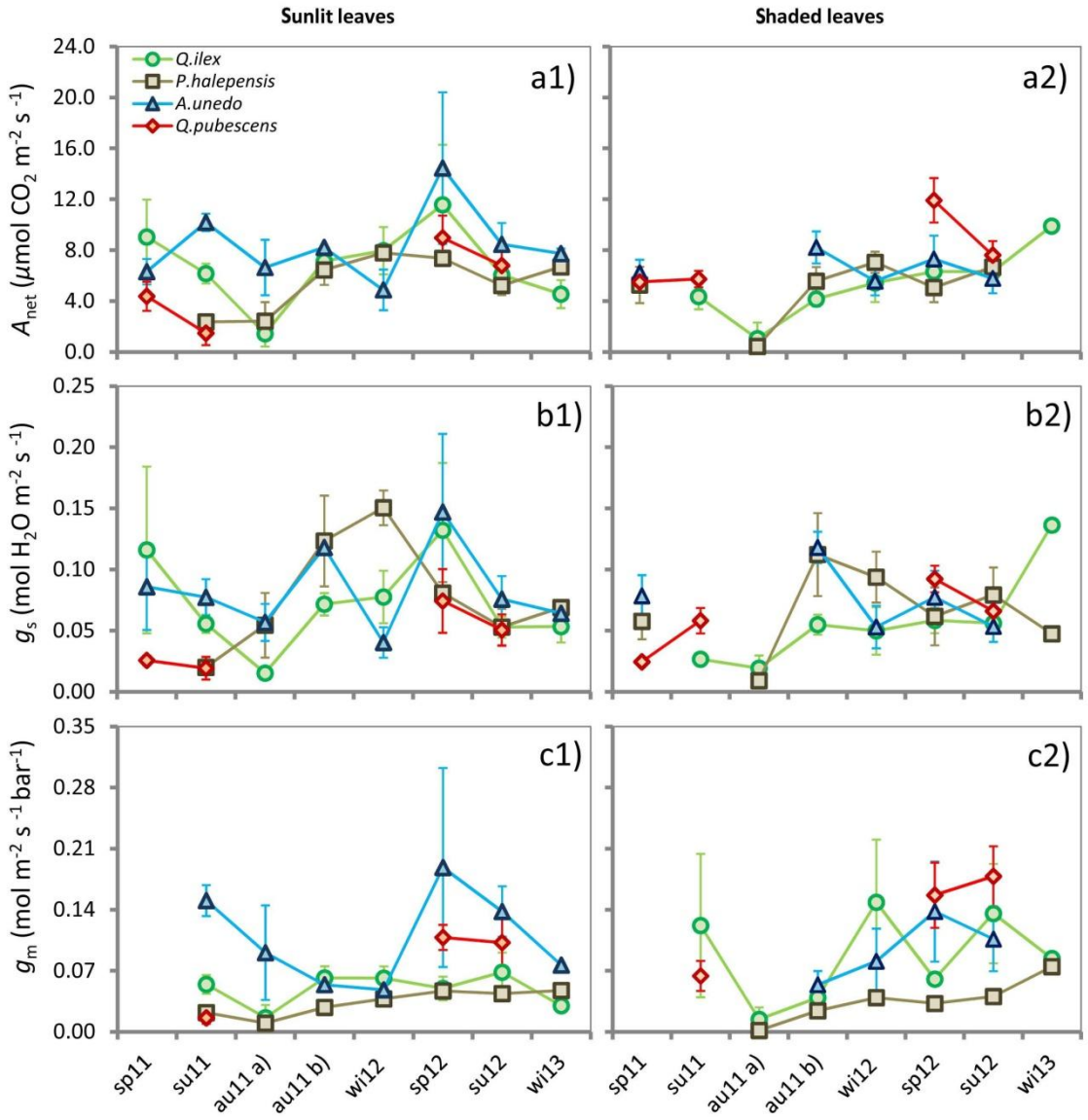


**Fig. 4.** Line graphs depicting seasonal changes of a) net assimilation ($A_{net}$), b) stomatal conductance ($g_s$), and c) mesophyll conductance ($g_m$) for *Q. ilex*, *P. halepensis*, *A. unedo*, and *Q. pubescens* in sunlit (1) and shaded (2) leaves. Seasonal campaigns were conducted in spring 2011 (sp11), summer 2011 (su11), autumn 2011[a] (au11 a), autumn 2011[b] (au11b), winter 2012 (wi12), spring 2012 (sp12), summer 2012 (su12), and winter 2013 (wi13). Missing data points were due to limitations of labour and equipment. Vertical bars indicate standard errors of the means ($n$ = 3-5).

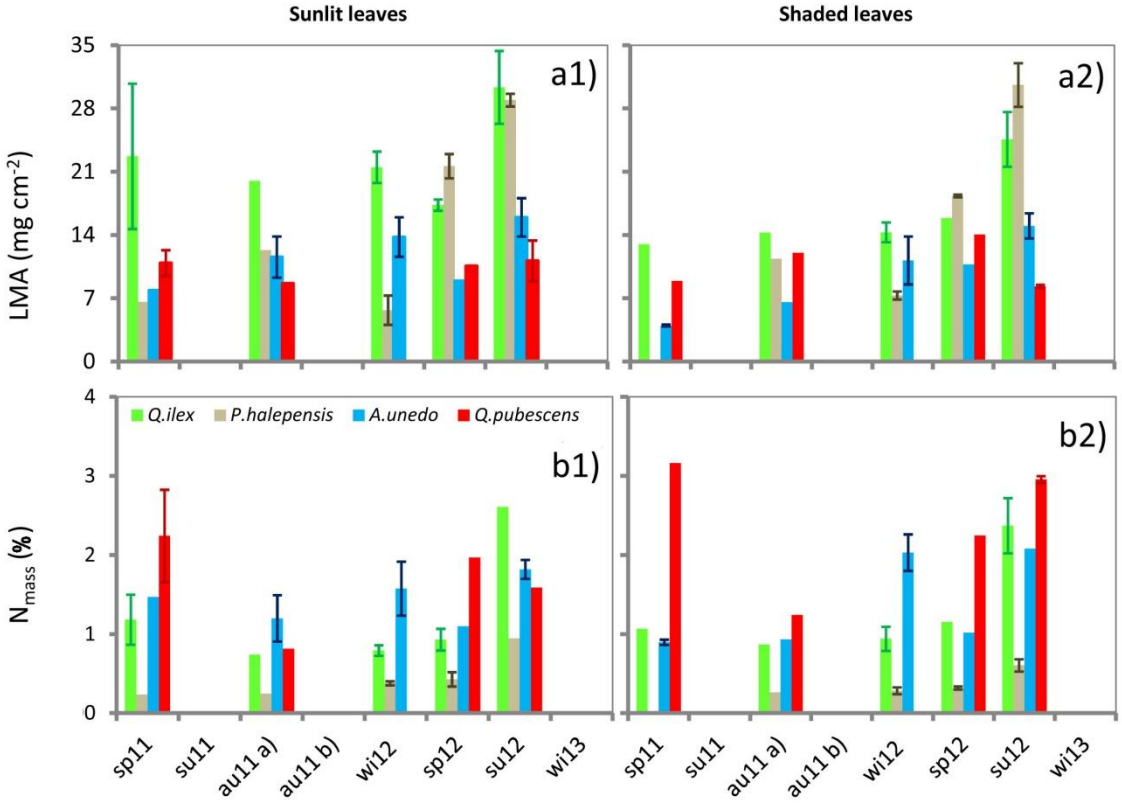


**Fig. 5.** Bar charts depicting seasonal changes of a) leaf mass per area (LMA) and b) percentage of nitrogen content per unit leaf mass ($N_{mass}$) for *Q. ilex*, *P. halepensis*, *A. unedo*, and *Q. pubescens* in sunlit (1) and shaded (2) leaves. Error bars indicate standard errors of the means ($n$ = 3-5).

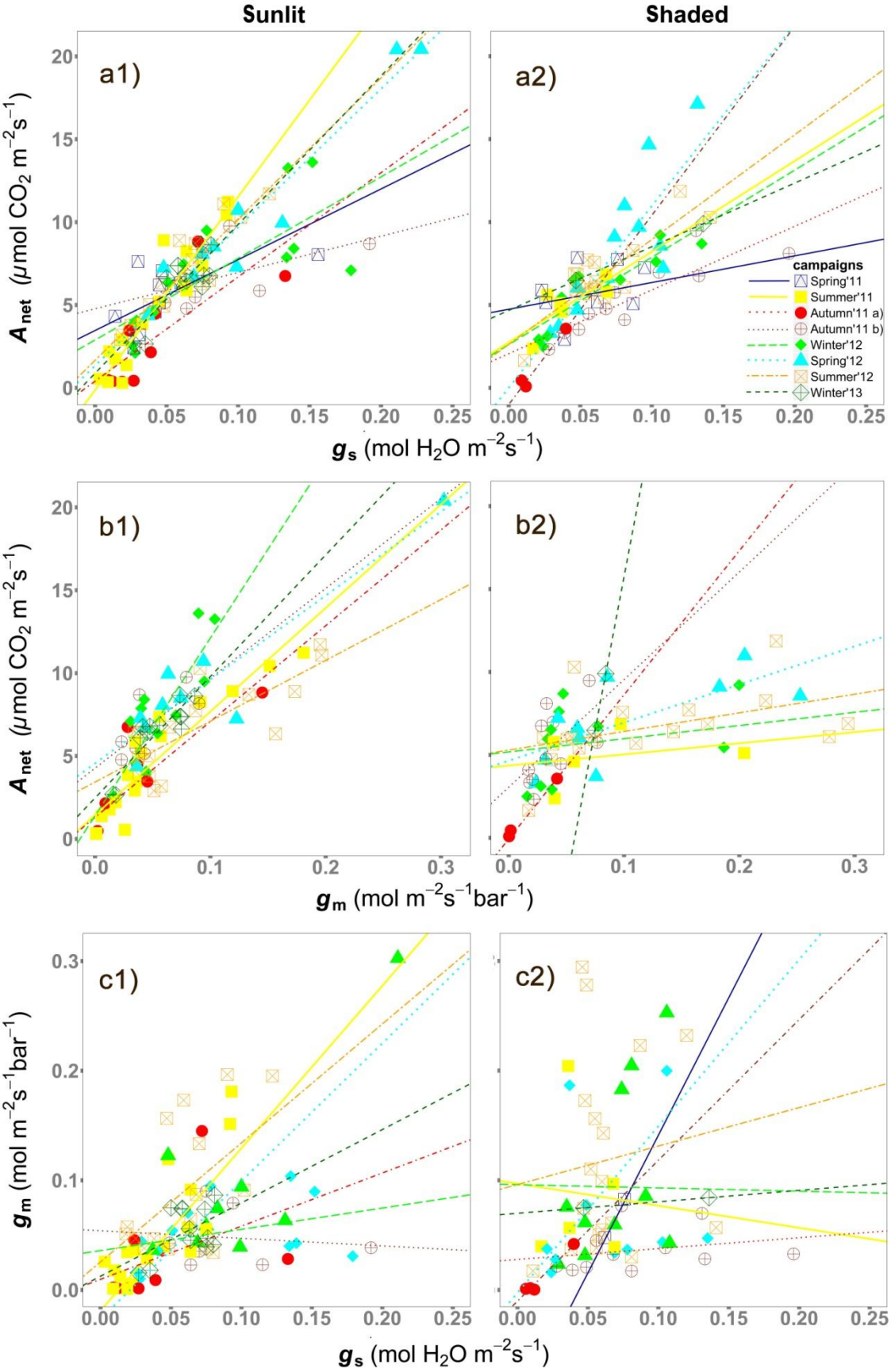


**Fig 6**. Seasonal changes of the relationships between a) net assimilation ($A_{net}$) and stomatal conductance ($g_s$), b) $A_{net}$ and mesophyll conductance ($g_m$), and c) $g_m$ and $g_s$ in sunlit (1) and shaded (2) leaves. The

regression lines represent the seasonal changes across species. For regression equations see Table S1-3. The relationships are shown as a thin solid line for spring 2011, short dashes for summer 2011, dots-dashes for autumn 2011[a)], small dots for autumn 2011[b)], dashes for winter 2012, large dots for spring 2012, large dots-dashes for summer 2012, and a thick solid line for winter 2013. Statistical differences in the slopes between seasonal campaigns were tested by ANCOVAs.

**Fig 7.** Seasonal changes of the relationships between a) the maximum electron-transport rate ($J_{max}$) and the maximum carboxylation rate ($V_{c,max}$) and b) the electron-transport rate from chlorophyllic fluorescence ($J_{amb}$) and net assimilation ($A_{net}$) at ambient $CO_2$ concentrations and saturating light in sunlit (a) and shaded (b) leaves. The regression lines represent the seasonal changes across species

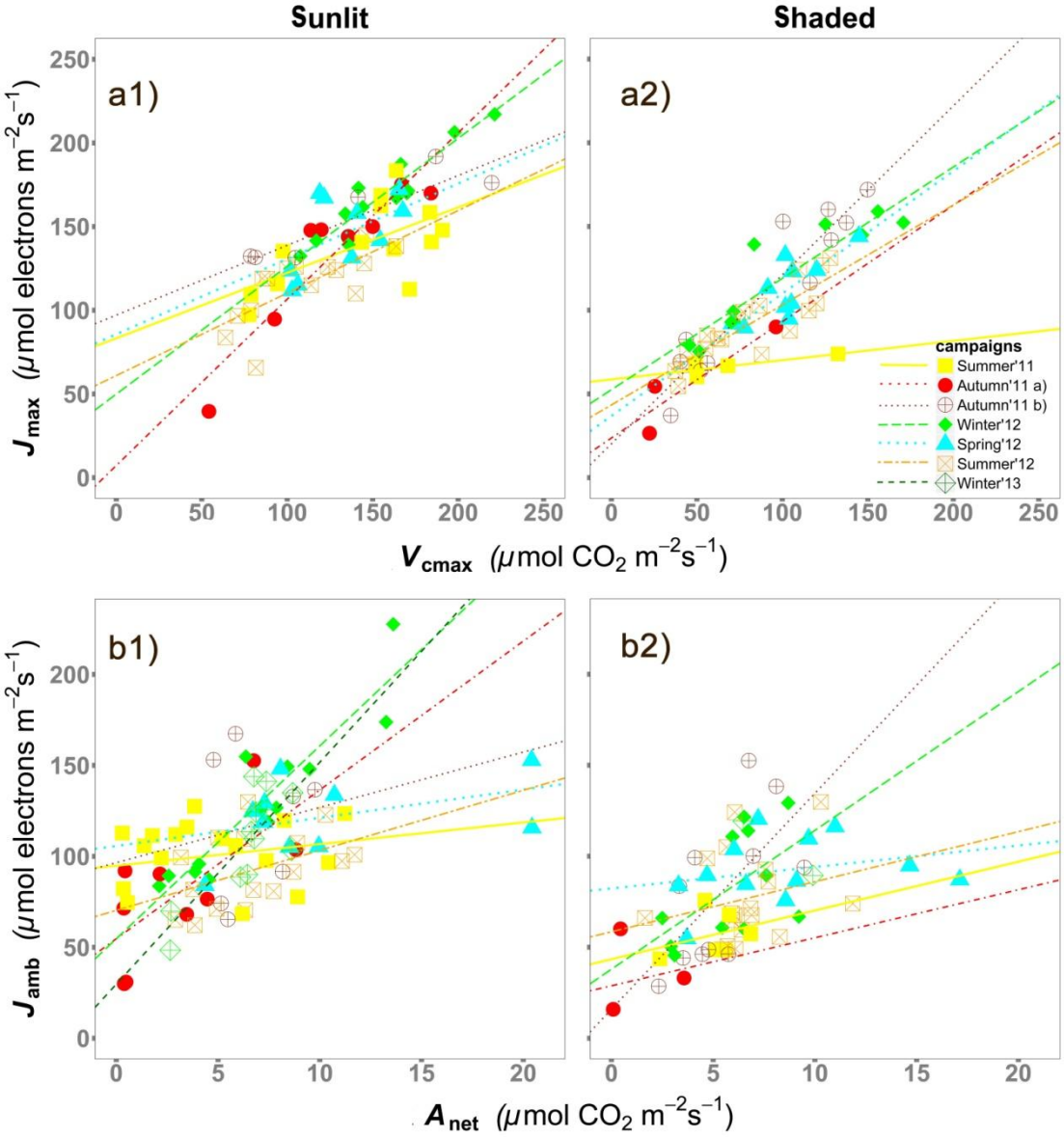


. For regression equations see Table S4-5. The relationships are shown as a short dashed line for summer 2011, dots-dashes for autumn 2011[a)], small dots for autumn 2011[b)], dashes for winter 2012, large dots for spring 2012, large dots-dashes for summer 2012, and a thick solid line for winter 2013. The campaign of spring 2011 was dismissed due to limitations in the chlorophyll fluorescence equipment.

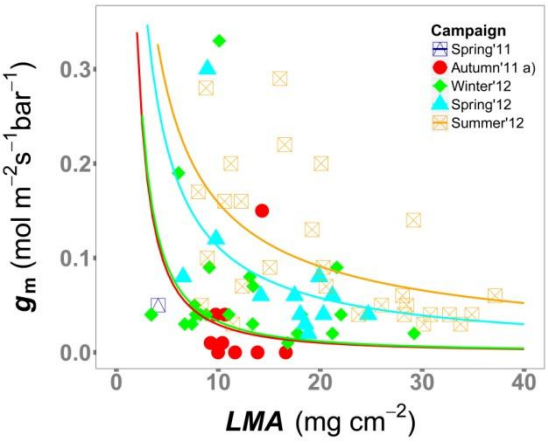


**Fig 8**. Seasonal changes of the relationship for all species and leaf positions between a) mesophyll conductance ($g_m$) and leaf mass per area (LMA).We used a subset of morphological and photosynthetic data. Non-linear regression lines of the form $y = x^{-b}$ were fitted to the data. The upper curve is for summer 2012 ($b$ = 0.800), the middle curve is for spring 2012 ($b$ = 0.953) and the lower two overlaying curves are for autumn 2011[a)] ($b$ = 1.533) and winter 2012 ($b$ = 1.486).